Korean J. Chem. Eng., **26**(1), 42-47 (2009)

LB energy-saving high temperature shift catalyst and its adsorption thermodynamics

Lingchao Wei*,,†, Fu'An Wang*, Yi Liu**, and Yongli Chai****

*College of Chemical Engineering, Zhengzhou University, Zhengzhou 450002, Henan, China
**Henan Key Laboratory of Chemical Catalysis, Zhengzhou 450052, Henan, China
(*Received 11 March 2008 • accepted 24 June 2008*)

Abstract−This study prepared an LB energy-saving high temperature shift catalyst by optimizing its prepare parameters with artificial neural network, and measured its catalytic activities at various steam-gas ratios. It shows that the LB catalyst performs well at a lower steam-gas ratio. The chromatographic retention parameters of CO, CO_2, and H_2O on LB catalyst were experimentally determined by means of inverse gas chromatography (IGC). Adsorption enthalpies, Gibbs adsorption free energies and adsorption entropies of different gases were estimated by their retention volumes in infinite dilution region. The interaction parameters (χ) between absorbate gases and LB catalyst were calculated according to Flory-Huggins theory, and were inversely linear with temperature. The thermodynamics mechanism of the adsorption process was discussed from the view of the microcosmic factors of molecular structure and thermodynamic properties.

Key words: Energy-saving High Temperature Shift Catalyst, Catalytic Activity, Adsorption Thermodynamics, Inverse Gas Chromatography, Water Gas Shift

INTRODUCTION

In the process of producing hydrogen or synthesis gas, it is usual to have a step where carbon monoxide conversion occurs, the so-called water gas shift reaction (WGSR). This reaction is a crucial step in many industrial processes, such as the synthesis of ammonia, methyl alcohol, dimethyl ether, hydrogen, city coal gas, etc. The carbon monoxide conversion to carbon dioxide in the presence of steam is a reversible and exothermic reaction. In practice, catalysts are frequently employed in the WGSR to facilitate the performance of the reaction. Furthermore, according to the reaction temperature or catalyst type, the WGSR falls into a high temperature shift reaction (HTSR) and a low temperature shift reaction. The traditional catalysts commonly used in HTSR are iron-chromium-based catalysts, which have to be reduced with hydrogen or semi-water gas before being used. As the reduction condition is rigorous and the molar steam-gas ratio must be high, the energy consumption is tremendous. As a result of the skyrocketing price of crude oil and energy in recent years, an energy-saving high temperature shift catalyst is of interest to the chemical industry and has been widely investigated. It not only can work at low molar steam-gas ratio, but also can reduce Fischer-Tropsch outgrowth. The LB energy-saving high temperature shift catalyst [1,2] is one of the novel catalysts; it performs very well in energy-saving ammonia plants where the molar steam-gas ratio is 2.75 or even lower.

In the gas-solid heterogeneous catalytic reaction, the adsorption process is a critical step. The interactions between the probes and the solid can be determined by the measurement of the retention time or the retention volume of the probes near zero surface coverage, which makes the characterization of the solid surface possible. For many years gas-solid chromatography has been used to study adsorption and catalytic reactions due to its advantages compared with static methods. Inverse gas chromatography (IGC) can detect the adsorption performance of gas on solid granule surface effectively, accurately and sensitively. In recent years, IGC has been successfully used to evaluate the dispersive characteristics of oxide surface, and proved to be highly effective in evaluating the surface properties of solid powders (alumina, smectite, talc, Au/-Al_2O_3, carbon black, Kaolinite, illite, etc.) [3-8]. The objective of this study is to determine the adsorption thermodynamics of gases, such as CO, CO_2 and H_2O, on the LB energy-saving high temperature shift catalyst; and it intends to pave a way to the study of its industrial applications, process optimization and catalytic mechanism.

†To whom correspondence should be addressed.
E-mail: miaoyin928@sina.com

EXPERIMENTS AND METHODS

1. Catalyst Preparation and Activity Determination

The LB energy-saving high temperature shift catalyst was prepared by the nitric acid method to avoid sulfur, and could be used in large-scale energy-saving ammonia plants. During the catalyst preparation, the precursors were an aqueous ferric solution prepared by nitric acid, CrO_3, $Ce(NO_3)_3$ and $La(NO_3)_3$. First, Cr^{6+} was reduced to Cr^{3+} in a reduction process. The Fe-Cr-Ce-La multi-element composite oxides were co-precipitated with ammonia solution as the precipitator. The slurry was filtered and washed several times with deionized water, and then dried at 393.2 K. The solid deposition was impregnated with a $Cu(NH_3)_4CO_3$ solution, dried, calcined and molded into pellets of ϕ5.0×4.5 mm. Finally, the pellets were crushed and sieved to grains of 1.40-2.00 mm (10-14 mesh) in diameter for the catalytic test, and of 0.20-0.30 mm (60-80 mesh) for the chromatographic measurement.

In previous research, many preparation parameters, such as the content of oxides, calcinations temperature and time, reaction pH value, and the solution's concentration, were found to possibly influence the catalytic activities. The relation between preparation pa-

rameters and catalytic activities is one of the most complex relations due to the strong nonlinearity. The artificial neural network (ANN) is an empirical modeling tool that is an artificial intelligence approach in which biological neurons are represented by a mathematical model. ANN offers a fast, efficient, accurate and cost-effective paradigm of process modeling. The ability of ANN to capture any complex input-output relationships only from limited data is very valuable in manufacturing processes where huge experimental data for the process modeling is difficult and expensive to obtain. Over the last 10 years, ANNs have been extensively studied to present process models, and their use in industry has been rapidly growing.

We developed a precise and robust back-propagation artificial neural network (BPANN) model to generate a catalytic activity predictor. The key influential factors on activities of the LB energy-saving high temperature shift catalyst were regarded as characteristic input vectors and catalytic activities as output vectors. The orthogonal tests results were divided into train group and prediction group, Neural Network Toolbox in MATLAB and Bayesian Automated Regularization Algorithm were utilized to build BPANN model, which can not only avoid that a network slides into the trap of partial minimum, but also enhances the precision and the generalization of the network. The optimal preparation conditions to manufacture LB catalyst were obtained after simulations. The catalyst is a kind of multi-element composite oxide, which consists of CuO : 5.8%, CeO_2 : 0.76%, Cr_2O_3 : 8.6%, La_2O_3 : 1.0%, Fe_2O_3 : the rest.

The catalytic activity test was performed at atmospheric pressure in a stainless-steel tube reactor equipped with a thermocouple in the catalyst bed. The catalyst (10-14 mesh, 5.0 g, about 5.0 ml) was put into the fixed-bed reactor. The space velocity of water gas, controlled by the mass flow controllers (Brook 5850E, USA), was 2,000 $mL \cdot h^{-1} \cdot g^{-1}$. The concentration of CO in water gas is 28.0% (mol), and the water vapor was gained by forcing the gas to pass through two pressure-tight water baths in serial order. Before the experiments, the catalyst was reduced in H_2 at 673.2 K for 2 hours, then was heated to 773.2 K and kept for 15 hours in the water gas flow. At last the temperature was reduced to 623.2 K, steam-gas ratio was changed to 0.40, and the steam-carbon ratio was 1.43. The tests started after the operation conditions were stable for 2 hours. The inlet and outlet compositions were analyzed with an on-line gas chromatograph.

2. Catalyst Characterization

After pretreatment at 673.2 K in vacuum, the specific surface areas, pore volume and size distribution were measured with a Quantachrome NOVA2000 Automated Gas Sorption System using nitrogen as the adsorbate. The pool temperature was 77.35 K and the analysis time was 6-8 hours.

3. IGC Apparatus and Determination

Adsorption measurements employed a conventional gas chromatograph (SP 3420, Beijing Analysis Instruments Co., Ltd, China) with a thermal conductivity detector (TCD). It has a KYS-668 type gas chromatography data processor to memorize and calculate the experimental data automatically. The carrier gas was hydrogen (99.99%). 11.75 g of LB catalyst was directly filled into a Premium grade 304 stainless steel column under mechanical vibration and vacuum. The column is 1,950 mm in length and 3mm in inner diameter. Its two ends were plugged with silane-treated glass wool, and its inner wall was passivated to minimize its interference during the IGC experiment. The operating parameters include the column pressure, carrier gas flow rate, atmospheric pressure, and the environmental temperature. The flowrate at the detector outlet was measured with a calibrated soap-bubble flowmeter, which had an accuracy of ±0.02 mL. The pillar temperature was displayed automatically by the chromatograph, which had an accuracy of ±0.5 K. The inlet and outlet column pressure were measured with an manometer, whose precision is 2.0 kPa. CO, CO_2 and H_2 (PRAXAIR Company) all are 99.99% in purity. The water used was doubly treated with both distillation and deionization.

During the measurements the temperature range was 313.2- 473.2 K. The highest temperature of the experiment was less than 483.2 K to prevent the catalyst from being over-reduced by the carrier gas. Before the tests, the columns were kept stable in the GC system at 483.2 K for 3 hours under a hydrogen flow rate of 30 $mL \cdot min^{-1}$. And the catalyst was reduced by H_2. To minimize the contamination to the detector, the column outlet was not connected to the detector during the stabilization period. In order to make the surface of the catalyst clean, the catalyst were exposed to a flow of H_2 (30 $mL \cdot min^{-1}$) for 2 hours at 373.2 K to remove the possible compounds adsorbed on the catalyst surface until the basic line of the recorder became smooth. When the temperature changed, the measurement started after the temperature was stable for at least 0.5 hours. Samples were injected into column with a 10 μL syringe. At least three replicate measurements were conducted under each temperature, and the most dependable data were obtained on the basis of normal distribution theory and Soufen standard. The non-interacting gas (He) was injected in order to determine the dead-retention time of each column. The net specific retention volumes V_g ($mL \cdot g^{-1}$) of CO, CO_2, and H_2O on LB catalyst were calculated according the following equation (Eq. (1)),

$$V_g = \frac{t_R - t_M}{w} \frac{273.15}{T_0} \frac{P_0 - P_W}{P_0} Fj \quad (1)$$

Where t_R is the retention time (min) of the adsorbed gas, t_M is the zero retention reference time (min) of the non-absorbed probe such as helium, w is the weight (g) of the catalyst in the column, T_0 is the temperature (K) of the soap-bubble flowmeter, P_0 is the atmospheric pressure (kPa), P_w is the saturated vapor pressure (kPa) of the water under the temperature of the soap-bubble flowmeter, F is the flow rate ($mL \cdot min^{-1}$) of the carry gas exiting the column under the temperature of the soap-bubble flowmeter, and j is the James-Martin gas compressibility correction factor (Eq. (2)).

$$j = \frac{3(P_i/P_o)^2 - 1}{2(P_i/P_o)^3 - 1} \quad (2)$$

Where P_i is the inlet pressure (kPa) of column.

RESULTS AND DISCUSSION

1. Catalytic Behavior at Low Molar Steam-gas Ratio

The catalysts were prepared in the optimized preparation parameters. Their catalytic activities at various steam-gas ratios were measured and recorded after the temperature of the water baths was at steady status for 2 hours when the steam-gas ratio was changed. The space velocity of dry gas was controlled at 2,000 $mL \cdot h^{-1} \cdot g^{-1}$. The results are shown in Fig. 1.

Fig. 1 shows that the catalytic activity of LB catalyst increased with the increase of the stream-gas ratio first, then became stable at

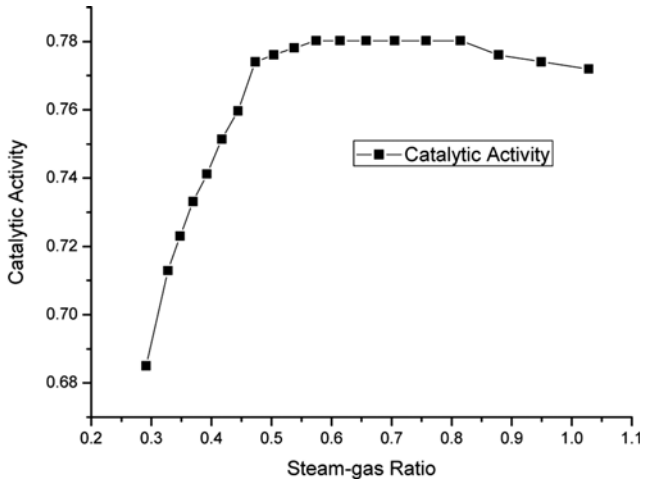

Fig. 1. The relation between catalytic activity and steam-gas ratio.

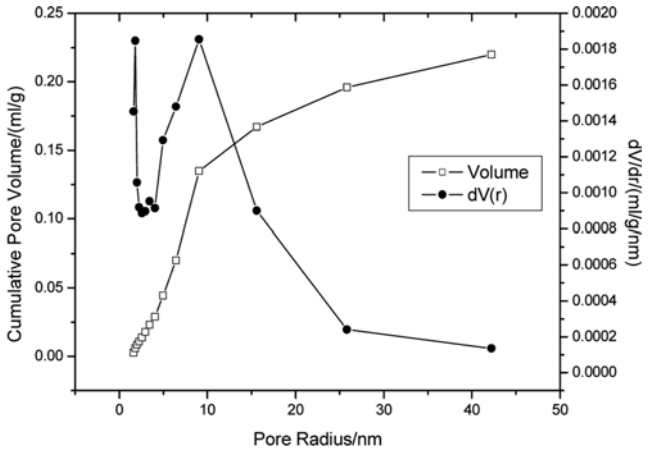

Fig. 2. The pore distribution of LB catalyst.

a wide range of steam-gas ratio, and began to descend slightly at the end. It indicates that LB catalyst has a good operating performance at low stream-gas ratio, and it works better at low stream-gas ratio than at higher ones. So the stream and energy consumption can be greatly reduced.

Fig. 1 also shows that the catalytic activity came to the maximum when the steam-gas ratio was 0.55 and the steam-carbon ratio was 1.53. According to catalysis theory, the steam is the reactant of the WGS reaction. So the conversion rate should increase with the increase of steam-gas ratio. But in fact, the conversion rate reached the maximum when the steam-gas ratio was 0.55, and kept steady until the steam-gas ratio was 0.93. During the steady period, the steam-carbon ratio was from 1.96 to 3.32, lower than 3.5 for traditional commercial catalysts in industrial ammonia plants. Even when the steam-gas ratio was 0.3 and the H_2O/CO was only 1.08, the catalytic activity of LB catalyst remarkably was 68.3%. And the reduction ratio R1=$(y_{CO}+y_{H_2})/(y_{CO_2}+y_{H_2O})$=(27.8+42)/(8+30)=1.84 [9], which was much bigger than the maximum reduction ratio 1.60 when the Fe-Cr HTS catalyst was reduced to iron. It indicates that LB catalyst had an excellent ability to resist being over-reduced. After the steady stage, the activity did not continue to increase with the increases of the steam-gas ratio, but began to fall slightly. One explanation is that LB catalyst has extremely strong ability to absorb and decompose the water molecule. The absorption and activation balance between water molecule and catalyst surface (or the reaction balance between the activated water molecules and activated CO molecules) is reached at lower steam-gas ratio. Too much water depresses the CO concentration in the gas mixture, and reduces the chance of CO molecule colliding with activated O. Therefore, the conversion decreases. LB catalyst has a better performance under low steam-gas ratio than under high steam-gas ratio.

The WGS reaction is mainly influenced by the adsorption and the activation of H_2O molecule. The catalyst has a good activity when the steam-gas ratio is at its normal range. When the concentration of steam decreases or the steam-gas ratio decreases, the time of water molecules staying on the catalyst surface still remains at a high level due to the significant adsorption ability of LB catalysts. Therefore H-O-bonding has more chance to be cleaved.

2. Pore Distribution and Specific Surface Area

The reduced LB catalyst was characterized with N_2 as the absorbate at 77.35 K. The pore distribution is shown in Fig. 2. The specific surface area of LB catalyst is 55.49 $m^2 \cdot g^{-1}$, the pore volume is 0.22 $mL \cdot g^{-1}$, the average pore radius is 7.99 nm, and the porosity is 0.5770.

According to IUPAC classification standard, the pores with a diameter less than 2 nm, between 2-50 nm, and bigger than 50 nm are generally defined as micropore, mesopore, and macropore, respectively. It is obvious that most pores in LB catalyst were mesopores, and a few were macropores.

3. The Net Specific Retention Volume

The net specific retention volume (V_g) is often expressed in the infinite dilution when the steady adsorption status between absorbate and catalyst is reached. Under the condition of infinite dilution, vapor molecules cover an extremely small fraction of the stationary phase surface so that the lateral interactions of the probe molecules can be neglected. In this study, the net specific retention volumes were determined at different injection amounts at the same temperature, and then were extrapolated to the net specific retention volume at the injection amount of zero. The net specific retention volumes of CO, CO_2 and H_2O on the LB catalyst measured at various temperatures in the experiments are listed in Table 1.

Table 1 shows that V_g of CO, CO_2 and H_2O increased in turn at

Table 1. The net specific retention volumes of CO, CO_2 and H_2O on the LB catalyst

T/K	CO	CO_2	T/K	CO	CO_2	H_2O
	$V_g/_{ml \cdot g^{-1}}$	$V_g/_{ml \cdot g^{-1}}$		$V_g/_{ml \cdot g^{-1}}$	$V_g/_{ml \cdot g^{-1}}$	$V_g/_{ml \cdot g^{-1}}$
313.2	0.5193	0.5336	413.2	0.4052	0.4117	163.7
323.2	0.5080	0.5139	423.2	0.3952	0.4008	155.2
333.2	0.4915	0.5020	433.2	0.3894	0.3895	137.5
343.2	0.4704	0.4816	443.2	0.3745	0.3888	128.3
353.2	0.4658	0.4763	453.2	0.3684	0.3786	121.8
363.2	0.4454	0.4548	463.2	0.3688	0.3737	113.4
373.2	0.4323	0.4485	473.2	0.3628	0.3627	109.4
383.2	0.4237	0.4333				
393.2	0.4150	0.4197	$\Delta H/kJ \cdot mol^{-1}$	−28.23	−29.07	−114.2
403.2	0.4131	0.4105	r^2	0.9970	0.9977	0.9934

the same temperature, V_g of CO and CO_2 were approximately the same, and V_g of H_2O was much larger than those of CO and CO_2.

4. Absorption Thermodynamic Property

The V_g of CO, CO_2 and H_2O decreased gradually with the rise of temperature. Thermodynamic data describing the adsorption process were derived from the dependence of specific retention volume on temperature. According to Clausius-CLapeyron equation, the dependence of $\ln V_g$ on T^{-1} in the given temperature range is

$$\ln(V_g) = I - \frac{\Delta H}{RT} \tag{3}$$

Where ΔH is the adsorption enthalpy ($kJ \cdot mol^{-1}$) of the absorbed gas on the catalyst, I is a constant, *T* is adsorption temperature (K), R is the ideal gas constant ($kJ \cdot mol^{-1} \cdot K^{-1}$). The plot of $\ln V_g$ versus 1/T is shown in Fig. 3. They are well linear correlated. The adsorption enthalpies of CO, CO_2 and H_2O on the LB catalyst calculated from Fig. 3 are listed in Table 1. The correlative coefficients r^2 are also summarized in Table 1. They are calculated with the data in Table 1 by the least squares method according to Eq. (3).

Shown in Table 1, the adsorption enthalpy ΔH of CO, CO_2 and H_2O on LB catalyst is negative. It indicates the adsorption process is exothermic and belongs to physical adsorption. The adsorption enthalpy ΔH of CO, CO_2 and H_2O increasing in turn, indicates that the interaction between the absorbate gas and catalyst also increases in turn.

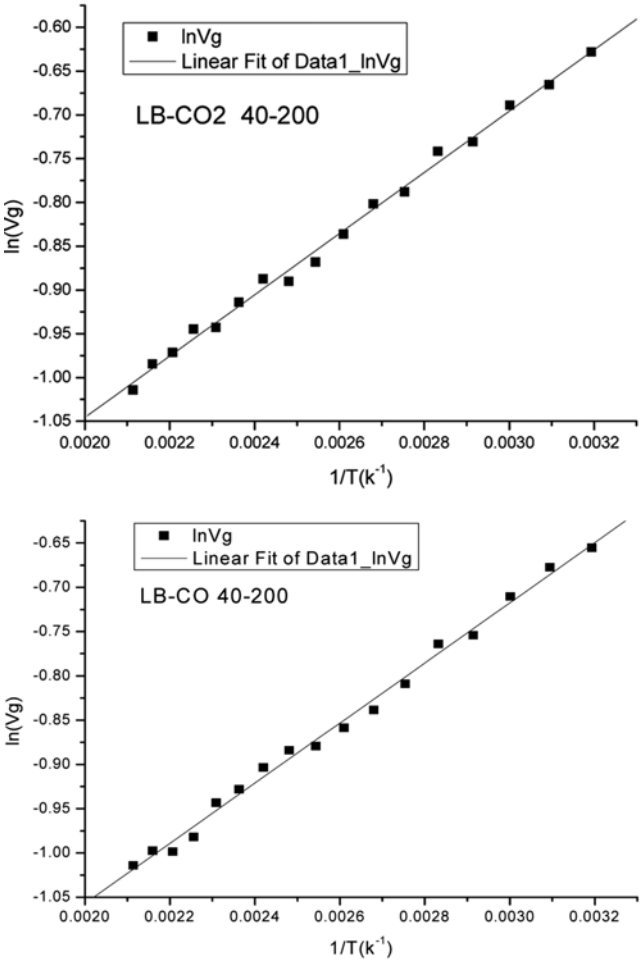

Fig. 3. The relation between the net retention volume of CO_2 and CO and adsorption temperature.

According to the theory of chromatography thermodynamics [10, 11], the microcosmic factors influence the adsorption enthalpy ΔH as follows:

$$\Delta H = B_1 \cdot \alpha_A + B_2 \cdot \mu_A^2 + B_3 + B_4 \tag{4}$$

Where B_1, B_2, B_3 and B_4 are the effect energy parameters of disperse force, electrostatic force, hydrogen bonding force and repulsive force, respectively; α_A and μ_A are the molecule polarization ratio and magnetic dipole moment of absorbate gas, respectively. In Eq. (4), −ΔH represents the interaction energy between the absorbed gas and LB catalyst. The main forces are the disperse force and electrostatic force for CO and CO_2 molecules. Hydrogen bonding force and repulsive force do not take place in this case. The magnetic dipole moment of CO molecules is 0.10 Debye, and that of CO_2 molecules is zero. However, the quadrupole moment of CO_2 molecules, which influences its thermodynamic properties intensively, is relatively big. Its polarization ratio is bigger than that of CO. So its adsorption enthalpy is slightly bigger than that of CO. Compared with CO and CO_2 molecules, water molecules are combinational molecules with big magnetic dipole moment and have hydrogen bonding force. Therefore, the adsorption enthalpy of H_2O is much bigger than that of CO and CO_2.

The Gibbs absorption free energy ΔG of absorbate gas in the inverse gas chromatography could be calculated in terms of the net specific retention volume according to the following equation [12]:

$$\Delta G^0 = -RT\ln\left(\frac{V_g P^O}{\pi^0 S_g w}\right) \tag{5}$$

Where π^0, 338 $\mu N \cdot m^{-1}$ [6,7], represents the spreading pressure of the adsorbed gas in the DeBoer standard state, w denotes the weight (g) of the catalyst in the chromatogram pillar, and S_g is the specific surface area ($m^2 \cdot g^{-1}$) of the catalyst. Data of ΔG for the solute-sorbent systems calculated from Eq. (5), at various temperatures, are given in Table 2.

Table 2 shows ΔG<0, which means the adsorption of CO, CO_2 and H_2O on the LB catalyst is spontaneous. Also, it reveals that CO, CO_2 and H_2O are easy to be adsorbed by the catalyst. The numerical value of Gibbs absorption free energy decreases with the increase of temperature, which suggests that the spontaneity of absorption process increases with temperature.

The adsorption entropy ΔS of the probe gas at zero coverage can be calculated with the following equation according to the Gibbs-Helmholtz equation based on the ΔH and ΔG in the adsorbing process,

$$\Delta S = (\Delta H - \Delta G)/T \tag{6}$$

The calculated absorption entropy ΔS of absorbate gas CO, CO_2 and H_2O on LB catalyst is listed in Table 2. In Table 2, the adsorption enthalpies were positive, which indicates that the adsorption is an enthalpy increase process [13]. According to the chromatogram thermodynamics theory, the microcosmic factors influence the adsorption entropy ΔS as follows [10,11],

$$\Delta S = R \cdot [(V_A/V_S) - \ln\beta] \tag{7}$$

Where V_A is the molar volume ($m^3 \cdot mol^{-1}$) of absorbate gas, V_S is

Table 2. Gibbs free energy, absorption entropy, interaction parameter of CO, CO_2 and H_2O

T/K	CO	CO_2	T/K	CO		CO_2		H_2O	
	$\Delta G/kJ\cdot mol^{-1}$	$\Delta G/kJ\cdot mol^{-1}$		$\Delta G/kJ\cdot mol^{-1}$	χ	$\Delta G/kJ\cdot mol^{-1}$	χ	$\Delta G/kJ\cdot mol^{-1}$	χ
313.2	−32.24	−32.31	413.2	−41.68	2.559	−41.74	2.038	−62.30	542.2
323.2	−33.21	−33.24	423.2	−42.60	2.581	−42.65	2.050	−63.62	552.0
333.2	−34.15	−34.20	433.2	−43.56	2.593	−43.56	2.064	−64.69	561.6
343.2	−35.05	−35.11	443.2	−44.42	2.629	−44.56	2.053	−65.92	570.7
353.2	−36.04	−36.10	453.2	−45.36	2.634	−45.46	2.068	−67.21	579.3
363.2	−36.92	−36.99	463.2	−46.36	2.640	−46.42	2.070	−68.42	586.8
373.2	−37.85	−37.96	473.2	−47.30	2.654	−47.30	2.089	−69.76	593.5
383.2	−38.80	−38.87							
393.2	−39.74	−39.78							
403.2	−40.74	−40.72	$\Delta S/J\cdot mol^{-1}\cdot K^{-1}$	93.95		93.86		123.1	

the molar volume ($m^3\cdot mol^{-1}$) of the catalyst, and β is phase ratio (the cubage ratio of the flow phase to the fixation phase in the chromatogram system). ΔS reflects the effect of molecule structure and configuration. The reason why ΔS>0 is that the relative molecule quality and the relative molecule volume of H_2 are less than those of CO, CO_2 and H_2O in the inverse phase gas chromatography. After being adsorbed on the catalyst, the movement of CO, CO_2 and H_2O molecules is regular than that of H_2. In other words, the movement of the molecules on the catalyst is less free than that of H_2. So the absorption entropy decreased when CO, CO_2, and H_2O molecules were absorbed on catalyst. But at the same time, the rearrangement of surface molecules might cause a large number of H_2 molecules leaving the surface of the catalyst. As the size of H_2 molecules is very small, the desorption of H_2 molecules changes their status from the distribution on the surface of catalyst in good order to free movement. Thus, it results in an increase in the degree of freedom and a considerable increase in the disorder of the system. Therefore, the entropy in this process increases greatly and the entropy of absorption is large. As a result, the total absorption entropy of the process in which the catalyst adsorbs CO, CO_2 and H_2O molecules is positive.

5. The Interaction Parameter between Absorbate Gas and LB Catalyst

According to the Flory-Huggins theory, the interaction parameter χ between absorbate gases and LB catalyst could be calculated according to the following equation [14]:

$$\chi = \ln\frac{273.15RV_s}{P_1^0V_gV_A} + \frac{V_A}{M_2V_S} - \frac{P_1^0(B_{11}-V_A)}{RT} - 1 \quad (8)$$

Where P_1^0 is the saturated vapor pressure (kPa) of absorbate gas, B_{11} is the second virial coefficient ($m^3\cdot mol^{-1}$) of absorbate gas, M_2 is the molecular weight ($g\cdot mol^{-1}$) of LB catalyst. The interaction parameters between the absorbate gases and LB catalyst are listed in Table 2. The relations between the interaction parameters of the absorbate gases and temperature are shown in Fig. 4.

Shown from Table 2, the interaction parameters between the absorbate gas CO, CO_2 and LB catalyst is small, while the interaction parameter between the water and the catalyst is big. That all of the χ are bigger than 0.5 indicates that there is only physical adsorption between the catalyst and the gases.

According to Ito and Guillet [15], the interaction parameter is linear with 1/T within a certain temperature range. In Fig. 4 the linear relation is obvious, but the changes of the interaction parameters of CO, CO_2 with temperature are not obvious. The interaction parameter of water increases observably with the temperature.

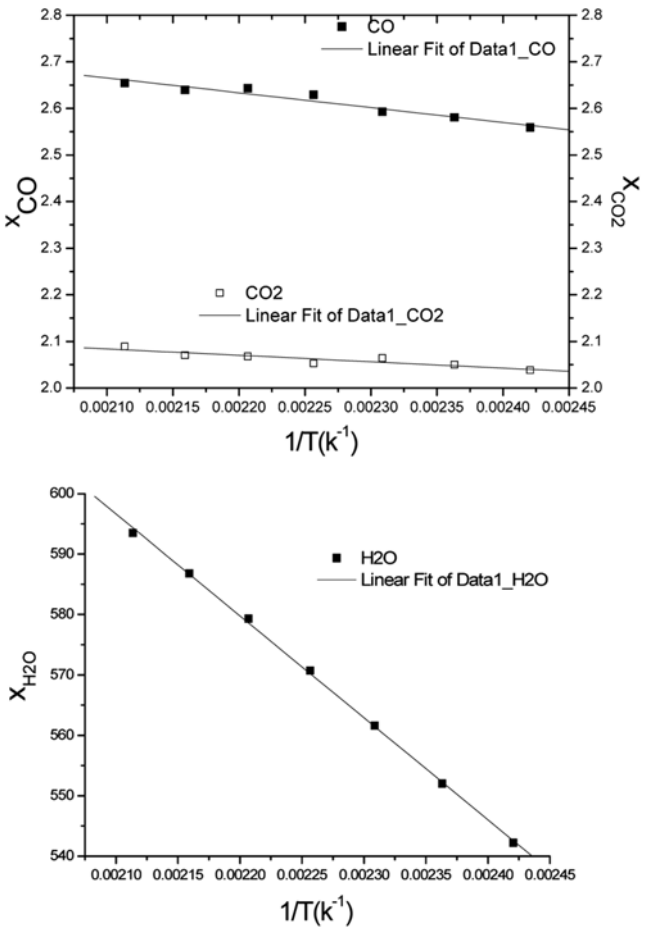

Fig. 4. The relation between interaction parameter and temperature.

CONCLUSIONS

This study prepared an LB energy-saving high temperature shift catalyst and measured its catalytic activity, specific surface area and

pore structure. The LB catalyst can be used at low steam-gas ratio and has strong ability to resist being over-reduced.

The net specific retention volumes V_g of CO, CO_2 and H_2O on LB catalyst were measured by the inverse gas chromatogram method. The relation between V_g and the temperature is linear. The absorption enthalpy ΔH, Gibbs absorption free energy ΔG, absorption entropy ΔS of CO, CO_2 and H_2O on LB catalyst were calculated in terms of the V_g at different temperatures. ΔH<0, ΔG<0, and ΔS>0 suggests that the absorption on the LB catalyst is an exothermic, spontaneous, and, entropy increase process.

The absorption thermodynamics was discussed based on the interaction parameters and chromatogram processing thermodynamics.

ACKNOWLEDGMENTS

The financial support of the National Development and Reform Commission of China in "2005 State Project of Major Industrial Technology Development" is gratefully acknowledged.

NOMENCLATURE

B_1 : disperse force
B_2 : electrostatic force
B_3 : hydrogen bonding force
B_4 : repulsive force
B_{11} : second virial coefficient [$m^3 \cdot mol^{-1}$]
F : flow rate [$mL \cdot min^{-1}$]
I : constant
j : James-Martin gas compressibility correction factor
M_2 : molecular weight [$g \cdot mol^{-1}$]
P_1^0 : saturated vapor pressure [kPa]
P_i : inlet column pressure [kPa]
P_0 : atmospheric pressure [kPa]
P_w : saturated vapor pressure of the water [kPa]
R : ideal gas constant [$J \cdot mol^{-1} \cdot K^{-1}$]
S_g : specific surface area [$m^2 \cdot g^{-1}$]
T : adsorption temperature [K]
T_0 : temperature of the soap-bubble flowmeter [K]
t_M : zero retention reference time [min]
t_R : retention time [min]
V_A : molar volume [$m^3 \cdot mol^{-1}$]
V_g : net specific retention volumes [$mL \cdot g^{-1}$]
V_S : molar volume [$m^3 \cdot mol^{-1}$]
w : weight [g]
ΔH : adsorption enthalpy [$kJ \cdot mol^{-1}$]
ΔG : Gibbs absorption free energy [$kJ \cdot mol^{-1}$]
ΔS : adsorption entropy [$J \cdot mol^{-1} \cdot K^{-1}$]
α_A : molecule polarization ratio
b : phase ratio
μ_A : magnetic dipole moment
π^0 : spreading pressure [338 $\mu N \cdot m^{-1}$]
c : interaction parameter

REFERENCES

1. L. C. Wei, F. A. Wang and Y. Liu, *Natural Gas Chemical Industry*, **2**, 11 (2006).
2. L. C. Wei, F. A. Wang and Y. Liu, *Chemical Reaction Engineering and Technology*, **6**, 497 (2006).
3. M. C. Gutierrez, J. Rubio and F. Rubio, *J. Chromatogr. A*, **845**, 53 (1999).
4. T. Hamieh, M. B. Fadlallah and J. Schultz, *J. Chromatogr. A*, **969**, 37 (2002).
5. G. Buckton, J. W. Dove and P. Davies, *Int. J. Pharm*., **1**, 13 (1999).
6. D. Gavril, A. Georgaka, V. Loukopoulos and G. Karaiskakis, *J. Chromatogr. A*, **1164**, 271 (2007).
7. Z. Witkiewicz, J. Oszczudlowski and M. Repelewicz, *J. Chromatogr. A*, **1062**, 155 (2005).
8. E. Fekete, J. Moczo and B. Pukanszky, *J. Colloid Interface Sci.*, **269**, 143 (2004).
9. J. W. Lywood and M. V. Twigg, Eur. Patent, 0,362,648 (1990).
10. P. Z. Lu, C. Z. Dai and X. M. Zhang, *The foundation of chromatogram theory*, The Science Press, Beijing (1997).
11. F. A. Wang and Y. L. Jiang, *Molecule thermodynamics and chromatogram retention*, Meteorology Press, Beijing (2001).
12. A. Aşkın and C. Bilgiç, *Chemical Engineering Journal*,**1-3**, 159 (2005).
13. C. L. Zhang, F. A. Wang and Y. Wang, *Korean J. Chem. Eng. Data*, **5**, 1563 (2007).
14. Q. C. Zou, J. Z. Zhang and Y. H. Zhang, *Chinese Journal of Analytical Chemistry*, **9**, 1012 (2001).
15. K. Ito and E. Guillet, *Macromolecules*, **12**, 1163 (1979).